Protein resistant surfaces: Comparison of acrylate graft polymers bearing oligo-ethylene oxide and phosphorylcholine side chains

Wei Feng and Shiping Zhu
Department of Chemical Engineering, McMaster University, 1280 Main Street West, Hamilton, Ontario, Canada L8S 4L7

Kazuhiko Ishihara
Department of Materials Engineering, School of Engineering, University of Tokyo, 7-3-1, Hongo, Bunkyo-ku, Tokyo, Japan 113-8656

John L. Brash[a)]
Department of Chemical Engineering, McMaster University, 1280 Main Street West, Hamilton, Ontario, Canada L8S 4L7

(Received 19 January 2006; accepted 17 February 2006; published 19 April 2006)

The objective of this work was to compare poly(ethylene glycol) (PEG) and phosphorylcholine (PC) moieties as surface modifiers with respect to their ability to inhibit protein adsorption. Surfaces were prepared by graft polymerization of the methacrylate monomers oligo(ethylene glycol) methyl ether methacrylate (OEGMA, MW 300, PEG side chains of length $n=4.5$) and 2-methacryloyloxyethyl phosphorylcholine (MPC, MW 295). The grafted polymers thus contained short PEG chains and PC, respectively, as side groups. Grafting on silicon was carried out using surface-initiated atom transfer radical polymerization (ATRP). Graft density was controlled via the surface density of the ATRP initiator, and chain length of the grafts was controlled via the ratio of monomer to sacrificial initiator. The grafted surfaces were characterized by water contact angle, x-ray photoelectron spectroscopy, and atomic force microscopy. The effect of graft density and chain length on fibrinogen adsorption from buffer was investigated using radio labeling methods. Adsorption to both MPC- and OEGMA-grafted surfaces was found to decrease with increasing graft density and chain length. Adsorption on the MPC and OEGMA surfaces for a given chain length and density was essentially the same. Very low adsorption levels of the order of 7 ng/cm^2 were seen on the most resistant surfaces. The effect of protein size on resistance to adsorption was studied using binary solutions of lysozyme (MW 14 600) and fibrinogen (MW 340 000). Adsorption levels in these experiments were also greatly reduced on the grafted surfaces compared to the control surfaces. It was concluded that at the lowest graft density, both proteins had unrestricted access to the substrate, and the relative affinities of the proteins for the substrate (higher affinity of fibrinogen) determined the composition of the layer. At the highest graft density also, where the adsorption of both proteins was very low, no preference for one or the other protein was evident, suggesting that adsorption did not involve penetration of the grafts and was occurring at the outer surface of the graft layer. It thus seems likely that preference among different proteins based on ability to penetrate the graft layer would occur, if at all, at a grafting density intermediate between 0.1 and 0.39 /cm^2. Again the MPC and OEGMA surfaces behaved similarly. It is suggested that the main determinant of the protein resistance of these surfaces is the "water barrier layer" resulting from their hydrophilic character. In turn the efficacy of the water barrier depends on the monomer density in the graft layer. [DOI: 10.1116/1.2187495]

I. INTRODUCTION

The phenomenon of protein adsorption to solid surfaces has attracted much attention in both industrial and academic circles for many years. In many situations it is desirable to minimize (ideally, prevent) protein adsorption. For example, in blood contacting applications, even a small quantity of adsorbed protein may give rise to the adhesion and activation of platelets, leading to thrombus generation. There is thus considerable interest in surfaces that might inhibit or prevent protein adsorption.[1–5] In this context, various water-soluble small molecules or polymers have been used to render surfaces hydrophilic and thereby suppress protein adsorption. Poly(ethylene glycol)[6,7] (PEG) and phosphorylcholine[8,9] (PC) moieties have been shown to be among the most effective surface modifiers for this purpose.

PEG, also referred to as poly(ethylene oxide) (PEO), is highly water soluble, and when dissolved in aqueous solvents, the chains have considerable flexibility and mobility, a large excluded volume, and generally strong interactions with water.[6] The protein resistance of PEG-grafted surfaces has been explained by "steric repulsion,"[10] caused essentially by the compression of the PEG chains as protein approaches

[a)]Author to whom correspondence should be addressed; electronic mail: brashjl@mcmaster.ca

the surface. This model seems reasonable for systems with relatively long PEG chains,[10–17] but less so for surfaces where the chains are short. Thus steric repulsion does not account well for the marked protein resistance of surfaces based on PEG grafts of length 2–6 ethylene oxide (EO) units.[18–22] For these short chain systems it is believed that the strong interactions of the EO moieties with water, including hydrogen bonding interactions, is responsible for their ability to resist protein adsorption.[20]

PEG-based surfaces having a variety of architectures including linear, star-like, and comb-like architectures have been investigated for their protein resistant properties. Linear and star-like architectures have been achieved by physical adsorption of polymers containing PEG chains,[16,23] or by covalent attachment of reactive PEG molecules to the surface ("grafting to" approach).[15,24–27] Comb-like architectures can be generated by graft polymerization of monomers with pendant EO side chains such as oligo(ethylene glycol) methyl ether methacrylate (OEGMA) and oligo(ethylene glycol) vinylbenzyl ("grafting from" approach).[28–32] Recently, surface-initiated living radical polymerization methods, especially surface-initiated atom transfer radical polymerization (ATRP), have been adapted for this purpose. For example, poly(OEGMA)-grafted surfaces on silicon,[33,34] gold,[35] and metal[36] substrates have been prepared by surface-initiated ATRP. The control afforded by these methods allows the generation of surfaces of well-defined graft density and chain length.

Phosphorylcholine (PC) is a major component of the outer surface of the erythrocyte membrane, and as such may be assumed to be nonthrombogenic. A biomimetic strategy for blood compatiblity based on the PC motif has thus been pursued by several groups,[8,9,37] and indeed it has been shown that PC-based surfaces are highly resistant to various proteins, blood cells, and bacteria.[9,37,38] The molecular mechanism of PC-mediated protein resistance is not clear, but it is believed that the highly hydrophilic PC head group binds a significant number of water molecules via electrostatic interactions, thus forming a hydration layer which inhibits interactions with proteins.[39,40]

PC-containing surfaces have been generated by forming PC-terminated self-assembled monolayers (SAMs) on gold or silicon substrates.[38,41–43] Carbon-chain polymers bearing PC side chains have also been developed as nonfouling coatings for biomaterials. The best known such polymers are based on the monomer 2-methacryloyloxyethyl phosphorylcholine (MPC). Direct surface grafting of MPC monomer from various substrates has been carried out either by conventional radical polymerization techniques[44–46] or by surface-initiated ATRP.[47,48] Recently, we prepared poly(MPC) grafted silicon surfaces by ATRP,[49,50] and showed that protein adsorption (both fibrinogen and lysozyme) was reduced by greater than 98% compared to controls.[51]

The objective of the present work was to compare PEG- and PC-based systems with respect to their effectiveness in preventing protein adsorption. Surfaces grafted with the methacrylate monomers, OEGMA (PEG side chains, $n=4.5$) and MPC, which contain, respectively, PEG and PC side chains of comparable size, were chosen as the basis for comparison. These monomers were graft polymerized from silicon by surface-initiated ATRP. Two important parameters believed to influence protein resistance, i.e., surface density and chain length of the grafts, were varied systematically by varying the surface density of the initiator and the ratio of monomer:sacrificial initiator, respectively. Single protein solutions of fibrinogen and binary solutions of fibrinogen and lysozyme were used in the protein adsorption experiments.

II. EXPERIMENTS

A. Materials

MPC was synthesized using a previously published procedure and recrystallized from acetonitrile.[52] OEGMA ($M_n \sim 300$) was purchased from Aldrich (Oakville, ON, Canada), distilled over CaH_2 under vacuum and stored frozen at $-15\ ^\circ C$. Fibrinogen (plasminogen free) was purchased from Calbiochem (La Jolla, CA), dialyzed against isotonic Tris buffer, pH 7.4, aliquoted, and stored at $-70\ ^\circ C$. Lysozyme (from chicken egg white) was obtained from Sigma Chemical Co. (St. Louis, MO) and used as received. Toluene (Caledon Laboratories Ltd., Georgetown, ON, Canada) was gently stirred over CaH_2 for 24 h and then distilled twice prior to use. All other reagents were obtained commercially and used without further purification. Double-sided polished silicon wafers (p-doped, ⟨100⟩-oriented, $10-20\ \Omega$ cm resistivity, 0.56 mm thickness) were purchased from University Wafer Company (Boston, MA) and cut into 5×5 mm pieces using a Micro Ace Series 3 dicer (Loadpoint Ltd., Swindon, England). De-ionized water purified by a Millipore water purification system to give a minimum resistivity of 18.0 MΩ cm was used in all experiments. Argon and nitrogen were of ultrahigh purity (UHP) grade. The water-soluble ATRP initiator oligomeric methoxy polyethylene glycol 2-bromoisobutyrate (OEGBr), was synthesized according to a published procedure.[53]

B. Formation of mixed self-assembled monolayers (SAMs)

The cleaning procedures for silicon wafers and the synthesis of the surface-attachable ATRP initiator, 10-(2-bromo-2-methyl) propionyloxydecyltrichlorosilane (**1**), were as described previously.[54] Mixed SAMs of **1** and dodecyltrichlorosilane (diluting agent, **2**) were formed on the silicon wafer surfaces by immersing freshly cleaned silicon wafers in mixed solutions of **1** and **2** in dry toluene solution for 18 h at room temperature. The mole fraction of **1** ranged from 1% to 100%. The wafers were removed from the solution, subjected to ultrasonication for 30 min in dry toluene, and rinsed sequentially with toluene and methanol (HPLC grade) to remove physisorbed initiator and diluting agent, and then dried under a nitrogen stream.

C. Surface-initiated ATRP of MPC and OEGMA

The surface-initiated polymerizations of MPC and OEGMA via ATRP were carried out as described previously.[33,49] OEGBr and ethyl 2-bromoisobutyrate (EBiB) were used as sacrificial initiators for MPC and OEGMA, respectively. In a typical run with OEGMA as the monomer, a sealed 10 ml pear-shaped flask containing Cu(I)Br (11.5 mg, 0.08 mmol) and bipyridine (bpy, 25.0 mg, 0.16 mmol) was degassed and refilled with argon three times. A deoxygenated mixture of OEGMA (1.2 *g*, 4.0 mmol) and methanol (2 ml) was added via syringe under stirring. The resulting dark brown solution was degassed for 30 min and then transferred to a glovebox filled with dry UHP nitrogen. At this time, EBiB (11.7 μl, 0.08 mmol) was added to the stirred solution. The reaction mixture was then aliquoted into glass tubes that contained initiator-functionalized silicon wafers. Polymerization was performed at room temperature for 24 h to allow complete monomer conversion. Samples were removed from the glovebox, rinsed with methanol, sonicated in methanol for 30 min to remove any unattached polymer, rinsed again with methanol, and dried under a nitrogen stream. For poly(MPC) grafting, the same procedures were followed except that OEGBr was used as free (sacrificial) initiator.

Five different monomer:sacrificial initiator ratios, viz., 5:1, 10:1, 50:1, 100:1 and 200:1, were used to vary the chain length of grafts for both MPC and OEGMA. Surfaces are referred to as "*x*-*y*-*z*," where *x* is the graft type: poly-(OEGMA) or poly(MPC), *y* is the graft density (from 0.05 to 0.39 chains/nm^2), and *z* is the chain length (5, 10, 50, 100, 200 monomer units).

The number-average molecular weight of poly(MPC) and poly(OEGMA) produced by sacrificial initiator in solution was determined by gel permeation chromatography using a procedure developed by Ma *et al.*[55] The monomer conversion in solution was determined from proton nuclear magnetic resonance spectra of the reaction media (Bruker AC-P200 spectrometer, D_2O solvent).

D. Surface characterization

The thickness of the initiator SAMs and polymer layers on the silicon substrate was obtained by ellipsometry (Exacta 2000 ellipsometer, Waterloo Digital Electronics, Waterloo, ON, Canada) equipped with a He–Ne laser (632.8 nm). An incident angle of 70° was used for all measurements. Refractive index of 1.5 was used for the calculation of the thickness of SAMs and polymer layers. All measurements were conducted in air at room temperature. Data for a given surface are reported as the average of at least three replicate measurements.

X-ray photoelectron spectroscopy (XPS) (Leybold Max 200, magnesium anode nonmonochromatic source) was used to determine the surface chemical composition of unmodified and modified surfaces. Survey scans (0–1000 eV) were performed to identify constitutive elements. Low-resolution scans of the peaks corresponding to these elements provided their atomic concentrations. High-resolution C1s spectra were recorded to obtain more detailed information on the nature of the surface. Measurements were made at takeoff angles of 20° and 90° relative to the sample surface.

Static water contact angles were measured with a Ramé-Hart NRL goniometer (Mountain Lakes, NJ) at room temperature. Silicon wafers were rinsed in methanol and dried in a nitrogen stream immediately before measurement. Advancing and receding contact angles were measured using the sessile drop method.

Atomic force microscope (AFM) images were obtained with a Multimode Nanoscope IIIa machine (Digital Instruments Inc.) operated in tapping mode. The measurements were performed under ambient conditions using a standard tip at a scan rate of 1.0 Hz. Immediately prior to measurements, samples were rinsed with methanol and dried in an air stream. The root-mean-square (rms) surface roughness was calculated from the roughness profiles.

E. Graft density from ellipsometry measurements

Graft densities were estimated using Eq. (1)

$$\sigma = \frac{h\rho N_A}{M_n}, \tag{1}$$

where σ is the graft density (chains/nm^2), h is the layer thickness (nm) from ellipsometry measurements, ρ is the density of the grafted polymer layer (values of 1.30 and 1.15 g/cm^3 were used for poly(MPC)[48] and poly(OEGMA),[56] respectively), N_A is Avogadro's number, and M_n is the number-average molecular weight of the grafted polymer chains, assumed to be the same as that of polymer produced in solution by OEGBr or EBiB initiation. This assumption has been shown to be valid for poly(methylmethacrylate) grafted on polyethylene by surface-initiated ATRP.[57]

F. Protein adsorption

For adsorption from both single and binary protein solutions, procedures were as described previously.[51] Solutions (Tris-buffered saline, TBS, *p*H 7.4) for adsorption measurements contained 10% radio-labeled (^{125}I- or ^{131}I-) protein and 90% unlabeled protein. Only fibrinogen was used in the single protein experiments. Two molar ratios of lysozyme to fibrinogen, 1:1 and 10:1, at each of two total protein concentrations, 0.05 and 1.0 mg/ml, were used in the binary protein experiments.

Adsorption was conducted in Microtest™ 96-well tissue culture plates (Becton Dickinson, NJ). Each well contained 250 μl protein solution and adsorption was allowed to proceed for 2 h at room temperature. Following adsorption, the surfaces were immersed in fresh TBS for 5 min (three cycles) to remove solution and loosely adsorbed protein. The samples were placed in counting vials and their radioactivity was determined using a Wizard™ 3 in. 1480 Automatic

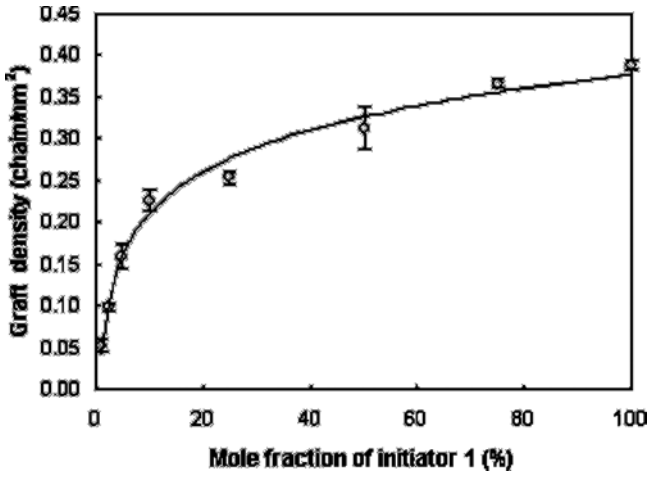

FIG. 1. Graft density of poly(OEGMA) layers as a function of mole fraction of **1** in the SAM at OEGMA/EBiB=100/1. Data are mean ±SD, $n \geqslant 3$. Curve is shown as a visual aid.

Gamma Counter (Perkin-Elmer Life Sciences). Typically, six replicate samples were run for each condition (surface, concentration, mol ratio).

III. RESULTS AND DISCUSSION

A. Preparation of polymer-grafted silicon wafers

A schematic of surface-initiated ATRP as used in this work is shown in Scheme 1. Silicon wafers were first treated with the initiator **1** or mixtures of **1** and the diluting agent **2** in dry toluene for 18 h at room temperature to produce mixed SAMs containing varying amounts of initiator. The mole fraction of initiator **1** in the SAMs ranged from 1% to 100%. The synthesis and characterization of these mixed SAMs has been reported previously.[50] The advancing water contact angle (θ_{adv}) decreased monotonically from 105° to 79° as the initiator mole fraction increased from 1% to 100%. Also, the bromine content (determined by XPS) increased with increasing mole fraction of **1**. These data indicate that the surface initiator density increased with increasing mole fraction of **1**.[50] As reported previously,[50] experiments on the surface-initiated ATRP of MPC using these mixed SAMs showed that the graft density of poly(MPC) increased rapidly with increasing mole fraction of **1** up to 25%. Beyond this value, the density increased more slowly and reached a limiting value of 0.39 chains/nm^2.

In the present work, we used the same methods to produce poly(OEGMA)-grafted silicon wafers of varying graft density using EBiB as sacrificial initiator. It is believed that the sacrificial initiator produces sufficient deactivating species in the initial stages of the ATRP process to maintain the "living" character of the polymerization.[57] The sacrificial initiator also allows control of the polymer chain length by varying the ratio of monomer:sacrificial initiator.[51,54]

The growth of the poly(OEGMA) layer as a function of initiator **1** mole fraction in the initiator layer at OEGMA:EBiB of 100:1 was measured by ellipsometry and used to calculate the graft density [Eq. (1)]. A number-average molecular weight M_n=23 200 g/mol and a bulk density of 1.15 g/cm^3,[56] were used in this calculation. The monomer concentration ([OEGMA]=2.0 M) and the molar ratios [EBiB]:[CuBr]:[bpy] (1:1:2) were constant in these experiments. As shown in Fig. 1, the graft density increased rapidly at low initiator concentration, and more slowly at high initiator concentration, with values ranging from 0.05 to 0.39 chains/nm^2 as the mole fraction of **1** increased from 1% to 100%. The graft density profile of poly(OEGMA) (Fig. 1) is similar to that of poly(MPC) observed in our previous work,[50] as expected on the basis of the similar size of the two monomers.

It should be noted that, for a given initiator mole fraction in the initiator layer, ATRP on these mixed SAMs resulted in similar graft densities for OEGMA and MPC. For investigation of protein resistance, surfaces based on two initiator mole fractions, viz., 2.5% and 100%, were selected. These produce, respectively, low (0.10 chains/nm^2) and high

TABLE I. Advancing (θ_{adv}) and receding (θ_{rec}) water contact angles on pristine and modified silicon wafer surfaces (room temperature).[a]

Surface	θ_{adv} (deg)	θ_{rec} (deg)	Surface	θ_{adv} (deg)	θ_{rec} (deg)
Si-2.5[b]	104±2	89±1	Si 100[c]	79±1	70±2
OEGMA-10-05	94±3	76±4	OEGMA-39-05	52±1	41±1
OEGMA-10-10	74±3	59±2	OEGMA-39-10	47±2	38±1
OEGMA-10-50	67±2	42±2	OEGMA-39-50	43±2	32±1
OEGMA-10-100	49±3	23±4	OEGMA-39-100	42±2	34±1
OEGMA-10-200	33±1	17±4	OEGMA-39-200	40±2	26±1
MPC-10-05	78±6	40±4	MPC-39-05	18±2	10±1
MPC-10-10	60±8	35±3	MPC-39-10	12±3	8±1
MPC-10-50	32±3	16±4	MPC-39-50	11±2	⋯
MPC-10-100	18±4	⋯[d]	MPC-39-100	9±2	⋯
MPC-10-200	12±3	⋯	MPC-39-200	9±2	⋯

[a]Data are mean±S.D., $n \geqslant 6$.
[b]Sites on substrate are 2.5% initiator species **1**, 97.5% inert species **2**. Graft density is 0.10 chain/nm^2.
[c]Sites on substrate are 100% initiator species **1**. Graft density is 0.39 chain/nm^2.
[d]Contact angle less than 7.0°.

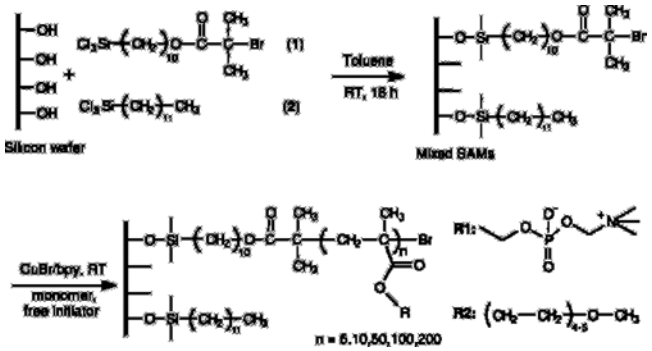

SCHEME 1. Synthesis of poly(OEGMA)- and poly(MPC)-grafted silicon with different graft densities and chain lengths

(0.39 chains/nm^2) graft density. Graft chain length was varied over the range of 5–200 monomer units by varying the ratio of monomer:sacrificial initiator.

B. Surface characterization

Advancing (θ_{adv}) and receding (θ_{rec}) water contact angle data for the initiator SAMs and the polymer grafted surfaces are listed in Table I. Prior to SAM formation, freshly cleaned silicon wafers showed an advancing water contact angle $<10°$. Angles of 104° and 79°, respectively, were found for the SAMs containing 2.5% and 100% initiator. The angles decreased after ATRP grafting, indicating an increase in hydrophilicity due to the grafted polymers. At low graft density, both θ_{adv} and θ_{rec} decreased with increasing chain length. For the high graft density surfaces, the angles decreased sharply in the short chain length range and became constant for chain length greater than 50. These results suggest that the surface was fully covered by polymer at high graft density and chain length greater than 50. As seen in Table I, poly(MPC)-grafted surfaces showed lower contact angles than poly(OEGMA) for a given graft density and chain length. For example, the θ_{adv} values were 40° and 9° for OEGMA-39-200 and MPC-39-200, respectively. The observed θ_{adv} values (40–45°) for fully covered poly(OEGMA) surfaces are similar to those reported for PEO-based surfaces on metal and Si substrates.[15,31,58]

Elemental composition data (from XPS experiments) on poly(MPC)-grafted silicon with low (0.10 chains/nm^2) and high (0.39 chains/nm^2) graft density and chain length from 5 to 200 monomer units were reported previously.[50] The P and N contents were shown to increase with increasing chain length and the P:N ratio was very close to the theoretical value of 1:1. The XPS data were in good agreement with the expected chemical composition of the grafted poly(MPC).

Table II presents elemental composition data for the poly(OEGMA)-grafted surfaces at takeoff angles of 90° and 20°. At both takeoff angles, the occurrence of grafting is indicated by a gradual increase in carbon and decrease in silicon with increasing layer thickness. For OEGMA-39-100 and OEGMA-39-200, the O and C contents are very close to their theoretical values. No Si was detected, indicating that the thickness of the grafted poly(OEGMA) layers was greater than the escape depth of the photoelectrons (~10 nm). Furthermore, analysis of the C1s high-resolution spectra demonstrated good agreement with the expected composition of poly(MPC) and poly(OEGMA). For example, the C1s scan of MPC-39-200 [Fig. 2(a)] was fitted with peaks at 284.8, 286.4, and 288.7 eV, corresponding to aliphatic (C–H/C–C), ether and amide (C–O/C–N), and ester (O=C–O) carbons respectively. The observed percentages of these components, i.e., 34.8%, 55.8%, and 9.4%, are consistent with the theoretical values of 27.2%, 63.7%, and 9.1% for poly(MPC). Similarly, the fitted C1s spectrum of OEGMA-39-200 indicated ratios C–C(H):C–O:O=C–O of 3.4:8.3:1.0 [Fig. 2(b)], again close to the expected values of 4.0:9.1:1.0.

The morphology of the grafted surfaces in the dry state was studied by AFM. Figure 3 shows typical images. At high graft density and chain length 100 [Figs. 3(a) and 3(b)] the poly(MPC) and poly(OEGMA) layers appear smooth with root-mean-square (rms) roughness of 0.34 and 0.30 nm, re-

TABLE II. Elemental composition of poly(OEGMA)-grafted silicon as determined by XPS.[a]

Surface	Graft layer thickness (nm)	Takeoff angle 90°			Takeoff angle 20°		
		Si	C	O	Si	C	O
OEGMA-10-05	0.5±0.2	33	42.1	24.9	15.2	60.1	24.7
OEGMA-10-10	0.9±0.4	32.3	44.4	23.3	17.9	62.3	19.8
OEGMA-10-50	2.0±0.6	27.5	51.6	20.9	14.3	66.3	19.4
OEGMA-10-100	3.4±0.5	14.6	59.0	26.4	7.7	65.3	27.0
OEGMA-10-200	6.5±0.6	10.2	62.4	27.4	4.9	68.5	26.6
OEGMA-39-05	1.2±0.4	23.0	50.8	26.2	10.4	64.0	25.6
OEGMA-39-10	2.3±0.3	19.9	52.2	27.9	8.3	68.4	23.3
OEGMA-39-50	6.7±0.4	11.2	61.6	27.2	3.6	69.2	27.2
OEGMA-39-100	13.0±0.2	···	70.1	29.9	···	69.9	30.1
OEGMA-39-200	25.8±0.8	···	70.7	29.3	···	68.5	31.5
Poly(OEGMA)[b]		···	68.3	31.7	···	68.3	31.7

[a]XPS data precision ~±5%. Data are atom %.
[b]Theoretical composition of poly(OEGMA).

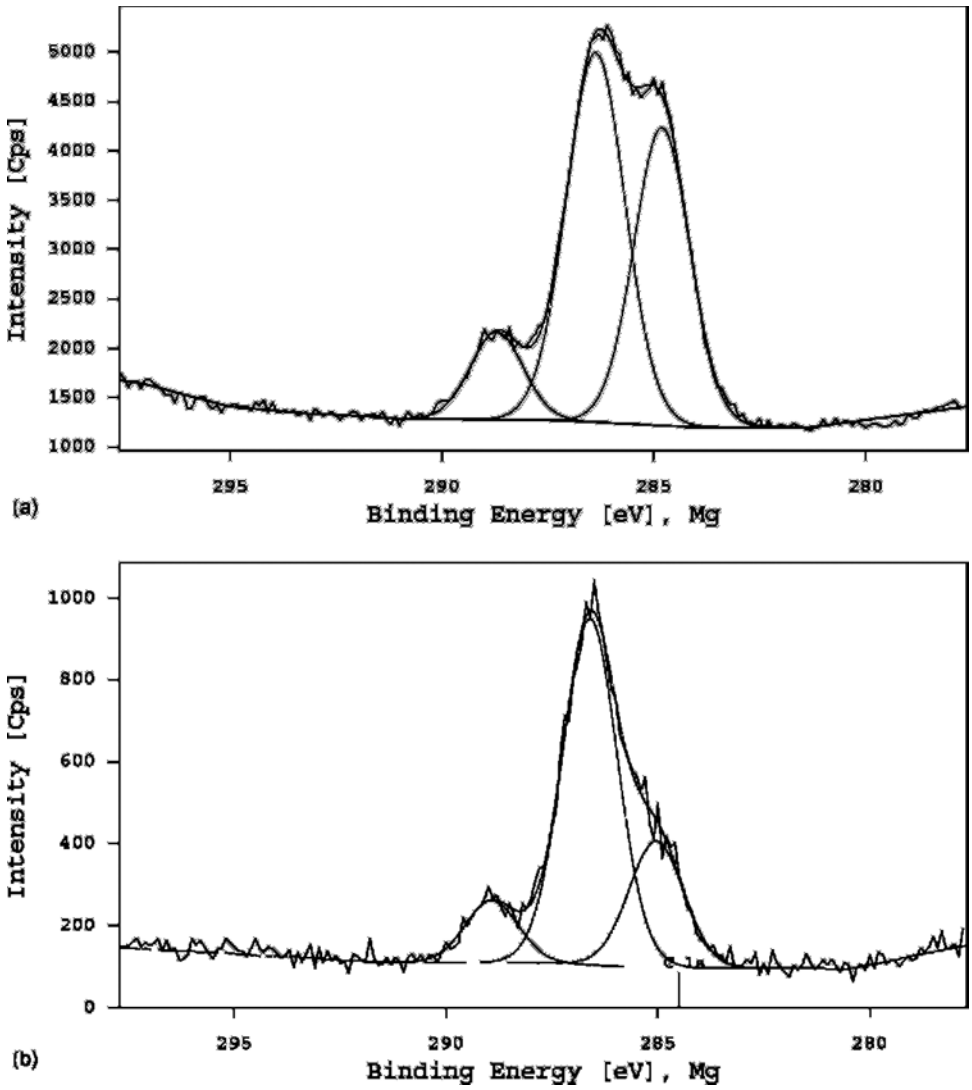

FIG. 2. Peak-fitted high-resolution C1s XPS spectra of: (a) MPC-39-200, and (b) OEGMA-39-200 surfaces at a takeoff angle of 90°.

spectively. At low graft density and chain length 100 [Figs. 3(c) and 3(d)] the surfaces appear rougher. The MPC surface shows rms roughness of 2.3 nm; the OEGMA is somewhat smoother with rms roughness 1.3 nm. At low graft density and chain length 200, the MPC surface shows rms roughness of 3.2 nm [Fig. 3(e)], whereas the OEGMA surface is relatively smooth [0.6 nm rms roughness, Fig. 3(f)]. The dissimilar surface morphologies of poly(MPC) and poly(OEGMA) at low graft density may indicate different molecular arrangements of the grafts on these two surfaces. Of course, it should be kept in mind that the morphology of the wet surfaces may be different, and it is in the wet state that the surfaces are encountered by proteins.

C. Adsorption of fibrinogen as single protein in buffer

Figure 4 shows adsorption data for fibrinogen on surfaces where the chain length was fixed at 100 monomer units and the graft density varied from 0.05 to 0.39 chains/nm^2. Adsorption decreased with increasing graft density for both poly(MPC)- and poly(OEGMA)-grafted surfaces, sharply in the lower graft density range and more gradually at higher graft density. No significant change was observed for graft densities greater than 0.31 chains/nm^2. Poly(MPC)- and poly(OEGMA)-grafted surfaces adsorbed similar quantities of fibrinogen at all graft densities. In this set of experiments we observed that the graft layer thickness (measured in the dry state) increased with graft density for both polymer types (data not shown) suggesting that the layers are in the brush regime over the entire range of graft densities used.[59]

The effect of graft chain length on fibrinogen adsorption at concentrations of 0.05 and 1.0 mg/ml is shown in Figs. 5(a) and 5(b), respectively. Two graft densities, viz., 0.10 and 0.39 chains/nm^2, were investigated. No significant difference was observed between the two control surfaces, Si-2.5 and Si-100, in which the SAMs contained 2.5 and 100% initiator respectively. At 0.05 mg/ml fibrinogen, the adsorbed amounts on the controls were $\sim$0.45 μg/cm^2, increasing to $\sim$0.57 μg/cm^2 at 1.0 mg/ml. These adsorbed amounts are in the range expected for close-packed mono-

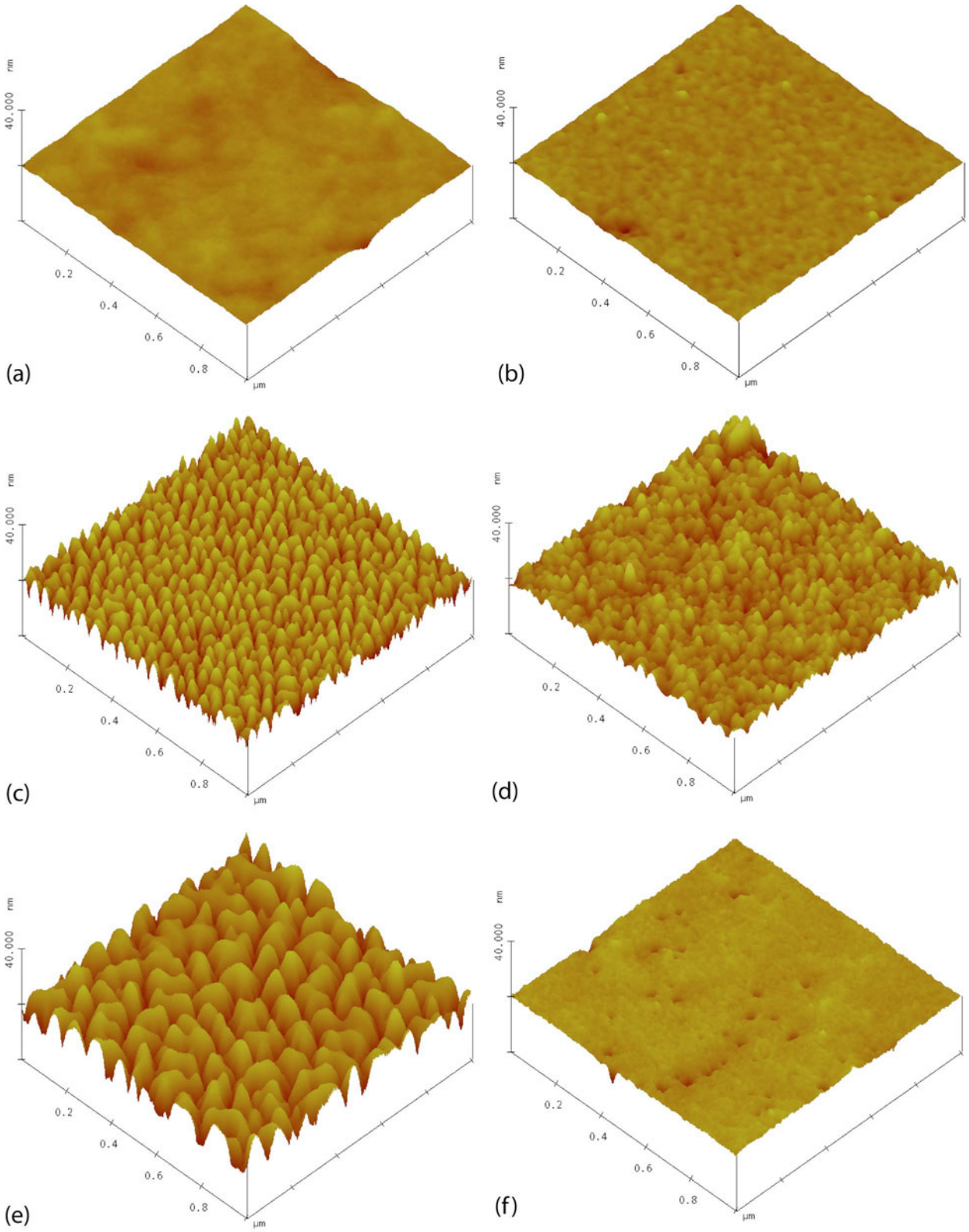

FIG. 3. Three-dimensional AFM images of poly(MPC)- and poly(OEGMA)-grafted silicon surfaces of varying graft density and chain length: (a) MPC-39-100; (b) OEGMA-39-100; (c) MPC-10-100; (d) OEGMA-10-100; (e) MPC-10-200; (f) OEGMA-10-200.

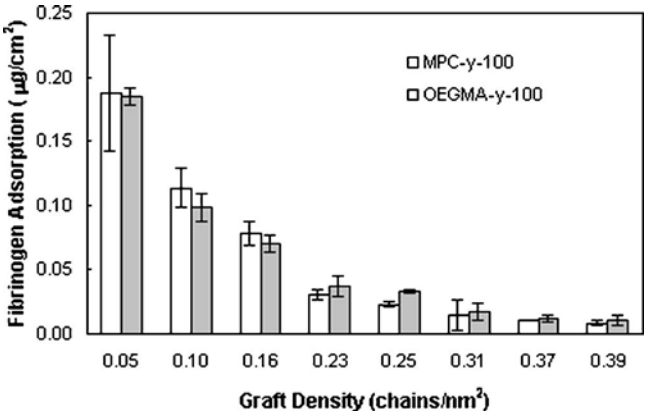

FIG. 4. Effect of graft density on fibrinogen adsorption to grafted silicon surfaces: graft chain length=100 monomer units. Fibrinogen concentration, 1 mg/ml in TBS buffer, pH 7.4. Data are mean ±SD, $n=6$. Adsorption time 2 h.

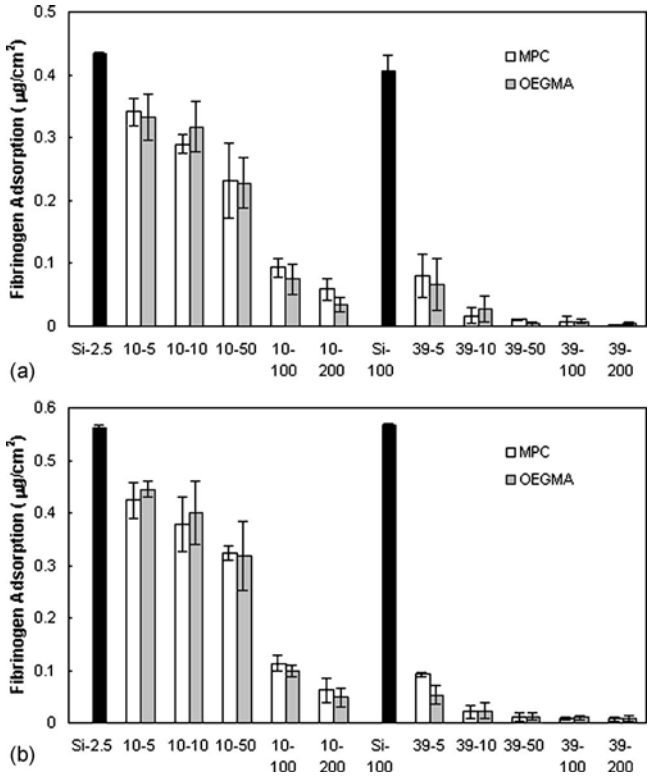

FIG. 5. Effect of chain length on fibrinogen adsorption to grafted silicon surfaces at graft densities of 0.10 and 0.39 chains/nm^2. Black bars are controls, i.e., Si 2.5 and Si 100. Fibrinogen concentration: (a) 0.05 mg/ml; (b) 1.0 mg/ml. Data are mean ±SD, $n=6$. Adsorption time 2 h.

layers (0.15 μg/cm^2 side on, 0.7 μg/cm^2 end on) and are in agreement with data reported previously for Si[50,51] and polystyrene substrates.[60] For the grafted surfaces, fibrinogen adsorption decreased with increasing chain length at both graft densities and fibrinogen concentrations. At a graft density of 0.10 chains/nm^2, adsorption decreased slightly with chain length in the range of 5–50 monomer units, and dramatically in the range of 100–200 monomer units. At the higher graft density of 0.39 chains/nm^2, adsorption decreased significantly over the short chain length range (from 5 to 10 monomer units), and only slightly over the longer chain length range. Based on these data, it appears that graft density is more important than graft chain length for protein resistance.

As seen in Figs. 5(a) and 5(b), the poly(MPC) and poly(OEGMA) grafted surfaces adsorbed similar amounts of fibrinogen for a given chain length and chain density. This result may be expected on the basis that the polymers should have similar solution properties in aqueous media like TBS, and thus should have similar chain conformation. The reductions in fibrinogen adsorption on the grafted surfaces versus the controls ranged from 20% to 99%, depending on the graft density and chain length. The surface concentrations on the MPC-39-200 and OEGMA-39-200 surfaces at 1.0 mg/ml were 7 ± 3 and 8 ± 5 ng/cm^2, respectively. These are very low values and are comparable to those seen on the most resistant PEG- and PC-based surfaces reported to date.[16,43]

D. Adsorption from binary solutions of fibrinogen and lysozyme

It was of interest to investigate whether the protein resistance of these grafted surfaces is dependent on protein size. It might be expected that for layers of relatively low graft density, resistance would be lower for smaller than for larger proteins, whereas at higher graft density, size would not be a factor. To address this question, adsorption from binary solutions of fibrinogen (MW 340 000, dimensions $9\times9\times46$ nm) and lysozyme (MW 14 600, dimensions $3\times3\times4.5$ nm) was studied. We reported previously[51] on poly(MPC)-grafted surfaces at high graft density and showed that these surfaces did not discriminate between lysozyme and fibrinogen. In the present work, we investigated poly(MPC)-grafted surfaces at low density and poly(OEGMA)-grafted surfaces at both low (0.10 chains/nm^2) and high (0.39 chains/nm^2) graft densities. The data for poly(MPC) surfaces at high graft density from our previous work are included here for comparison.

The data on adsorbed amounts are shown in Table III. It can be seen that the trends with respect to chain length and chain density were the same as for the single protein fibrinogen system. Also the absolute levels of fibrinogen adsorption at a given protein concentration were comparable to those for the single protein system.

Figures 6(a) and 6(b) show the lysozyme:fibrinogen (L:F) molar ratio in the adsorbed layer at a molar ratio of 1:1 in solution and total protein concentrations of 0.05 and 1.0 mg/ml, respectively. For the control surfaces (Si-2.5 and Si-100), the L:F ratio in the layer was approximately 1:1 at both total concentrations. For the grafted surfaces, the L:F ratios in the layers were also close to the solution value of 1:1 for both total concentrations [Figs. 6(a) and 6(b)], suggesting no preference of these surfaces for one or the other protein. The error bars for the data on these surfaces are large due to the large experimental errors on the measurements for the individual proteins (see Table III), and to error propagation when the ratios are calculated. The large experimental

TABLE III. Adsorbed protein amounts (ng/cm^2) in binary protein experiments at two molar ratios and two total protein concentrations.[a]

	Lys:Fib (1:1 molar ratio)				Lys:Fib (10:1 molar ratio)			
	0.05 (mg/ml)		1.0 (mg/ml)		0.05 (mg/ml)		1.0 (mg/ml)	
Surfaces	Lys	Fib	Lys	Fib	Lys	Fib	Lys	Fib
Si 2.5	14±1	481±43	23±1	698±26	40±3	361±37	92±7	503±26
Si 100	15±1	477±14	31±3	733±35	51±10	364±25	111±9	547±27
OEGMA-10-5	14±2	383±20	26±3	548±19	43±5	317±34	114±22	423±47
OEGMA-10-10	11±1	337±25	22±2	459±31	33±10	259±71	94±3	327±34
OEGMA-10-50	10±2	287±28	18±6	336±81	25±13	214±95	44±26	286±98
OEGMA-10-100	3±2	89±61	6±3	93±24	9±2	74±17	17±5	73±43
OEGMA-10-200	3±1	40±10	3±1	39±6	12±13	28±14	13±8	33±18
MPC-10-5	12±1	374±40	21±1	551±55	44±4	294±7	91±7	396±26
MPC-10-10	11±1	338±12	18±4	538±39	36±28	205±31	77±18	256±41
MPC-10-50	10±1	300±7	11±6	345±30	29±21	201±67	55±46	204±96
MPC-10-100	6±0.3	83±7	8±4	134±41	26±4	58±52	46±12	86±68
MPC-10-200	3±1	56±4	3±1	84±29	22±4	58±20	20±12	68±21
OEGMA-39-5	4±1	85±31	3±1	48±6	11±3	52±21	17±3	46±6
OEGMA-39-10	2±1	41±11	3±1	49±15	7±2	36±11	11±4	36±10
OEGMA-39-50	1±0.1	10±4	1±0.1	15±1	2±0.4	6±3	2±0.4	12±5
OEGMA-39-100	1±0.1	16±6	1±0.4	27±24	2±0.4	6±3	3±2	8±3
OEGMA-39-200	1±0.4	21±30	1±0.2	12±4	3±2	7±3	3±1	8±3
MPC-39-5[b]	2.2±1.4	62±46	4.0±1.6	54±23	10±4.4	56±37	22±11	54±28
MPC-39-10[b]	1.5±1.2	20±10	3.1±1.8	28±10	7.7±3.6	26±23	12±10	22±7
MPC-39-50[b]	0.6±0.2	8.6±2.4	1.7±0.8	17±7	2.2±1.0	8.7±5.4	8±4	18±6
MPC-39-100[b]	0.5±0.3	8.3±4.1	1.4±0.4	16±7	2.0±0.5	7.4±2.9	6±5	14±2
MPC-39-200[b]	0.5±0.3	10±7	1.0±0.3	18±7	3.0±0.6	9.2±2.4	4±1	16±3

[a]Data are mean±SD, $n \geqslant 6$.
[b]See Ref. 51.

errors are due to the very low absolute levels of adsorption on the grafted surfaces (see Table III), which, in the case of lysozyme, ranged from less than 1 to about 50 ng/cm^2.

Figure 7 shows data for the binary protein system at a solution molar ratio L:F=10:1. The ratios on the control surfaces were less than 10:1, suggesting that fibrinogen has a higher affinity than lysozyme for these surfaces. The L:F ratios on the grafted surfaces varied with graft density and chain length. At low graft density (0.10 chains/nm^2) and short chain length (5–50 monomer units), the L:F ratios in the adsorbed layers were less than 10:1 at both total protein concentrations, indicating that these surfaces adsorbed fibrinogen in preference to lysozyme. This is opposite to what might be expected based on the two adsorption modes on polymer brushes proposed by Halperin.[61] So-called primary adsorption occurs at or close to the substrate surface; it is considered important for small proteins and is predicted to decrease with increasing graft density. Secondary adsorption occurs at the outer surface of the graft layer; it is expected to be important for larger proteins and to decrease with increasing layer thickness. According to this model, lysozyme should more readily penetrate a low graft density brush than fibrinogen, and thus be able to adsorb at the graft-silicon interface. On this basis lysozyme should adsorb preferentially to fibrinogen. That the opposite trend is observed (Fig. 7) may be due to the fact that at this particular graft density, both proteins have unrestricted access to the substrate and thus the higher affinity of fibrinogen for the substrate determines the composition of the layer.

With increasing layer thickness (chain length) and graft density, the affinity of fibrinogen relative to lysozyme is expected to decrease. This prediction is in agreement with the data in Fig. 7 at low graft density (0.10 chains/nm^2) and long chain length (100 and 200 monomer units); the surface L:F ratios were higher than at short chain length, in some cases close to 10:1, the same as in solution. For the high graft density (0.39 chains/nm^2) OEGMA surfaces, the L:F ratios were similar in the surface and solution, suggesting that these surfaces resist the two proteins equally. A similar result was reported previously for high density MPC surfaces.[51] These results suggest that preference among different proteins based on ability to penetrate the graft layer would occur, it at all, at a grafting density intermediate between 0.10 and 0.39/cm^2. In general, from the binary data it appears that size is not a major factor for adsorption to these surfaces at the densities investigated, where the layers are in the brush regime. Furthermore, it seems likely that "residual" adsorption on the grafts may be occurring at the outer surface of the graft layer.

IV. CONCLUSIONS

The main objective of this work was to compare PEG- and PC-based surfaces with respect to their ability to inhibit protein adsorption. In this regard the data in Figs. 4 and 5 and Table III indicate that for a given graft chain length and density the adsorbed amounts are remarkably similar for both types of surface. This may indicate that protein resis-

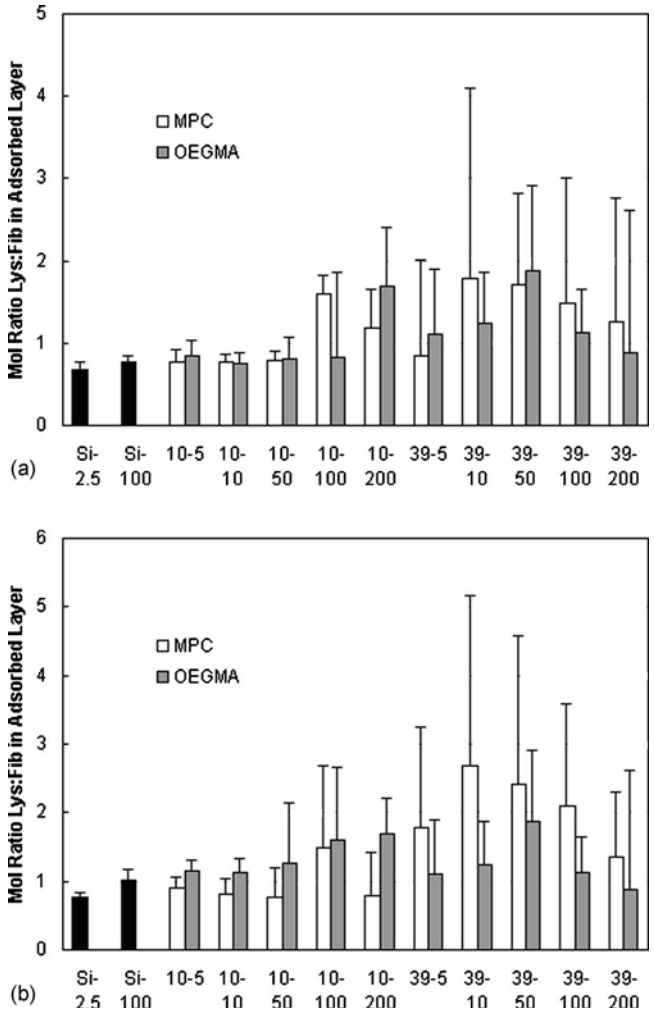

FIG. 6. Adsorption from binary lysozyme-fibrinogen solutions: molar ratio 1:1, TBS, *p*H 7.4. Data are molar ratio lysozyme:fibrinogen in the adsorbed layer at two total protein concentrations: (a) 0.05 mg/ml; (b) 1.0 mg/ml. Adsorption time 2 h.

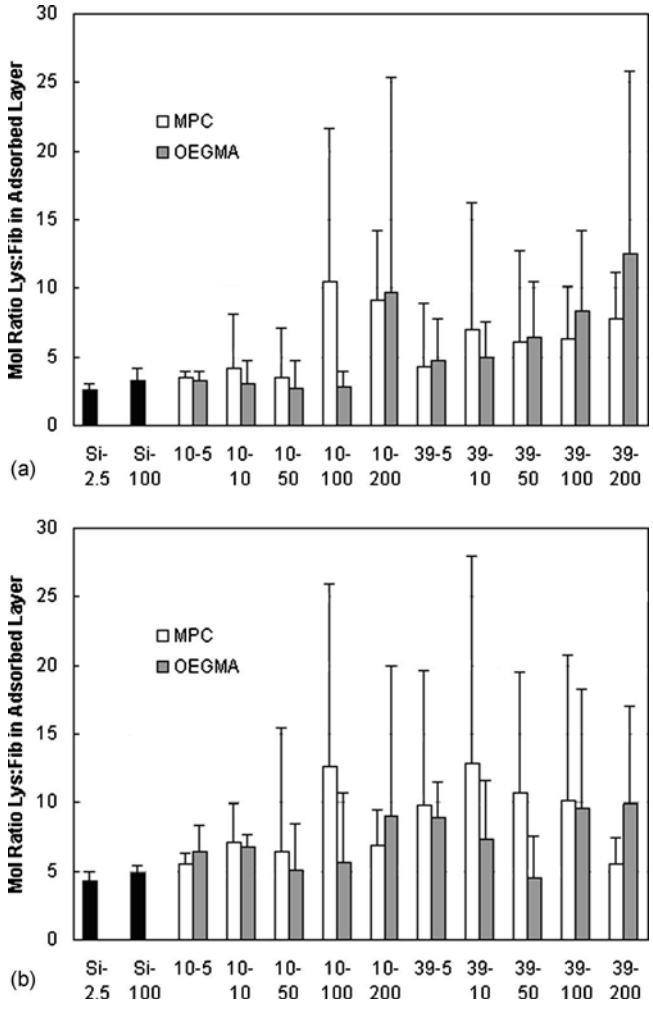

FIG. 7. Adsorption from binary lysozyme-fibrinogen solutions: molar ratio 10:1, TBS, *p*H 7.4. Data are molar ratio lysozyme:fibrinogen in the adsorbed layer at two total protein concentrations: (a) 0.05 mg/ml; (b) 1.0 mg/ml. Adsorption time 2 h.

tance is determined by the surface density of monomer units, i.e., ethylene oxide or MPC, since these are the same for both types of surface at the same chain length and density. Monomer density has been discussed as a determinant of protein resistance by Szleifer and others.[11,12,62] It appears to be a plausible concept to explain the results of the present investigation. Of course, it is not the monomers as such, but most likely the water layers associated with them that makes these surfaces protein resistant. If this is true then the results of this work suggest that the water layers on both types of surface are equally effective barriers to protein adsorption.

With regard to the fundamental mechanism of protein resistance, two ideas are current: steric exclusion based on chain flexibility of grafted polymers, and tightly held water (water barrier). The former has been advanced for flexible polymers like PEO of significant chain length; the latter for hydrophilic entities like PC and PEO, both of which bind water, albeit via electrostatic interactions in the case of MPC[43] and hydrogen bonding in the case of PEO.[63] In the present work both of the grafted polymers investigated have a carbon backbone and as such are not notably flexible. In addition in the case of OEGMA, the PEO side chains are short (4.5 average chain length) and are not likely to be capable of supporting steric exclusion to any significant extent. Therefore, the present results support the idea of a water barrier to account for the protein resistance of these surfaces.

ACKNOWLEDGMENTS

Financial support of this work by the Natural Sciences and Engineering Research Council of Canada (NSERC), the Canadian Institutes of Health Research (CIHR), and the Canada Foundation for Innovation (CFI) is gratefully acknowledged. W.F. is supported by an Ontario Graduate Scholarship for Science and Technology (OGSST).

[1]*Proteins at Interfaces II, Fundamentals and Applications*, edited by T. A. Horbett and J. L. Brash, ACS Symposium Series No. 602 (American Chemical Society, Washington, DC, 1995).
[2]D. G. Castner and B. D. Ratner, Surf. Sci. **500**, 28 (2002).
[3]J. L. Brash, J. Biomater. Sci., Polym. Ed. **11**, 1135 (2000).
[4]B. D. Ratner and S. J. Bryant, Annu. Rev. Biomed. Eng. **6**, 41 (2004).

[5]B. Kasemo, Surf. Sci. **500**, 656 (2002).
[6]J. H. Lee and J. D. Andrade, Prog. Polym. Sci. **20**, 1043 (1995).
[7]P. Vermette and L. Meagher, Colloids Surf., B **28**, 153 (2003).
[8]H. J. Mathieu, Y. Chevolot, L. Ruiz-Taylor, and D. Leonard, Adv. Polym. Sci. **162**, 1 (2003).
[9]Y. Iwasaki and K. Ishihara, Anal. Bioanal. Chem. **381**, 534 (2005).
[10]S. I. Jeon, J. H. Lee, J. D. Andrade, and P. G. De Gennes, J. Colloid Interface Sci. **142**, 149 (1991).
[11]I. Szleifer, Biophys. J. **72**, 595 (1997).
[12]T. McPherson, A. Kidane, I. Szleifer, and K. Park, Langmuir **14**, 176 (1998).
[13]M. Jonsson and H. O. Johansson, Colloids Surf., B **37**, 71 (2004).
[14]W. Norde and D. Gage, Langmuir **20**, 4162 (2004).
[15]L. D. Unsworth, H. Sheardown, and J. L. Brash, Langmuir **21**, 1036 (2005).
[16]G. L. Kenausis, J. Voros, D. L. Elbert, N. Huang, R. Hofer, L. Ruiz-Taylor, M. Textor, J. A. Hubbell, and N. D. Spencer, J. Phys. Chem. B **104**, 3298 (2000).
[17]J. G. Archambault and J. L. Brash, Colloids Surf., B **33**, 111 (2004).
[18]K. L. Prime and G. M. Whitesides, Science **252**, 1164 (1991).
[19]K. L. Prime and G. M. Whitesides, J. Am. Chem. Soc. **115**, 10174 (1993).
[20]P. Harder, M. Grunze, R. Dahint, G. M. Whitesides, and P. E. Laibinis, J. Phys. Chem. B **102**, 426 (1998).
[21]S. Herrwerth, W. Eck, S. Reinhardt, and M. Grunze, J. Am. Chem. Soc. **125**, 9359 (2003).
[22]D. V. Vanderah, H. La, J. Naff, V. Silin, and K. A. Rubinson, J. Am. Chem. Soc. **126**, 13639 (2004).
[23]J. H. Lee, J. Kopecek and J. D. Andrade, J. Biomed. Mater. Res. **23**, 351 (1989).
[24]S. B. Jo and K. Park, Biomaterials **21**, 605 (2000).
[25]S. J. Sofia, V. Premnath, and E. W. Merrill, Macromolecules **31**, 5059 (1998).
[26]J. Groll, Z. Ademovic, T. Ameringer, D. Klee, and M. Moeller, Biomacromolecules **6**, 956 (2005).
[27]J. Benesch, S. Svedhem, S. C. T. Svensson, R. Valiokas, B. Liedberg, and P. Tengvall, J. Biomater. Sci., Polym. Ed. **12**, 581 (2001).
[28]Y. Mori, S. Nagaoka, H. Takiuchi, T. Kikuchi, N. Noguchi, H. Tanzawa, and Y. Noishiki, Trans. ASAIO **28**, 459 (1982).
[29]S. Nagaoka and A. Nakao, Biomaterials **11**, 119 (1990).
[30]Y. H. Sun, A. S. Hoffman, and W. R. Gombotz, Polym. Prepr. (Am. Chem. Soc. Div. Polym. Chem.) **28**, 292 (1987).
[31]K. Fujimoto, H. Inoue, and Y. Ikada, J. Biomed. Mater. Res. **27**, 1559 (1993).
[32]F. Zhang, E. T. Kang, K. G. Neoh, P. Wang, and K. L. Tan, J. Biomed. Mater. Res. **56**, 324 (2001).
[33]W. Feng, R. X. Chen, J. L. Brash, and S. P. Zhu, Macromol. Rapid Commun. **26**, 1383 (2005).
[34]F. J. Xu, Y. L. Li, E. T. Kang, and K. G. Neoh, Biomacromolecules **6**, 1759 (2005).
[35]H. W. Ma, J. H. Hyun, P. Stiller, and A. Chilkoti, Adv. Mater. (Weinheim, Ger.) **16**, 338 (2004).
[36]X. W. Fan, L. J. Lin, J. L. Dalsin, and P. B. Messersmith, J. Am. Chem. Soc. **127**, 15843 (2005).
[37]A. L. Lewis, Colloids Surf., B **18**, 261 (2000).
[38]V. A. Tegoulia, W. S. Rao, A. T. Kalambur, J. F. Rabolt, and S. L. Cooper, Langmuir **17**, 4396 (2001).
[39]K. Ishihara, H. Nomura, T. Mihara, K. Kurita, Y. Iwasaki, and N. Nakabayashi, J. Biomed. Mater. Res. **39**, 323 (1998).
[40]H. Kitano, K. Sudo, K. Ichikawa, M. Ide, and K. Ishihara, J. Phys. Chem. B **104**, 11425 (2000).
[41]J. R. Lu, E. F. Murphy, T. J. Su, A. L. Lewis, P. W. Stratford, and S. K. Satija, Langmuir **17**, 3382 (2001).
[42]E. Ostuni, R. G. Chapman, R. E. Holmlin, S. Takayama, and G. M. Whitesides, Langmuir **17**, 5605 (2001).
[43]S. F. Chen, J. Zhang, L. Y. Li, and S. Y. Jiang, J. Am. Chem. Soc. **127**, 14473 (2005).
[44]A. Korematsu, Y. Takemoto, T. Nakaya, and H. Inoue, Biomaterials **23**, 263 (2002).
[45]K. Kim, C. Kim, and Y. Byun, Biomaterials **25**, 33 (2004).
[46]T. Moro, Y. Takatori, K. Ishihara, T. Konno, Y. Takigawa, T. Matsushita, U. I. Chung, K. Nakamura, and H. Kawaguchi, Nat. Mater. **3**, 829 (2004).
[47]X. Y. Chen and S. P. Armes, Adv. Mater. (Weinheim, Ger.) **15**, 1558 (2003).
[48]R. Iwata, P. Suk-In, V. P. Hoven, A. Takahara, K. Akiyoshi, and Y. Iwasaki, Biomacromolecules **5**, 2308 (2004).
[49]W. Feng, J. L. Brash, and S. P. Zhu, J. Polym. Sci., Part A: Polym. Chem. **42**, 2931 (2004).
[50]W. Feng, J. L. Brash, and S. P. Zhu, Biomaterials **27**, 847 (2006).
[51]W. Feng, S. P. Zhu, K. Ishihara, and J. L. Brash, Langmuir **21**, 5980 (2005).
[52]K. Ishihara, T. Ueda, and N. Nakabayashi, Polym. J. (Tokyo, Jpn.) **22**, 355 (1990).
[53]X. Jin, Y. Shen, and S. P. Zhu, Macromol. Mater. Eng. **288**, 925 (2003).
[54]M. Husseman, E. E. Malmstrom, M. McNamara, M. Mate, D. Mecerreyes, D. G. Benoit, J. L. Hedrick, P. Mansky, E. Huang, T. P. Russell, and C. J. Hawker, Macromolecules **32**, 1424 (1999).
[55]I. Y. Ma, E. J. Lobb, N. C. Billingham, S. P. Armes, A. L. Lewis, A. W. Lloyd, and J. Salvage, Macromolecules **35**, 9306 (2002).
[56]Density of poly(OEGMA) measured in house.
[57]K. Yamamoto, Y. Miwa, H. Tanaka, M. Sakaguchi, and S. Shimada, J. Polym. Sci., Part A: Polym. Chem. **40**, 3350 (2002).
[58]L. Andruzzi, W. Senaratne, A. Hexemer, E. D. Sheets, B. Ilic, E. J. Kramer, B. Baird, and C. K. Ober, Langmuir **21**, 2495 (2005).
[59]T. Wu, K. Efimenko, and J. Genzer, J. Am. Chem. Soc. **124**, 9394 (2002).
[60]J. Kim and G. A. Somorjai, J. Am. Chem. Soc. **12**, 3150 (2003).
[61]A. Halperin, Langmuir **15**, 2525 (1999).
[62]S. Pasche, M. Textor, L. Meagher, N. D. Spencer, and H. J. Griesser, Langmuir **21**, 6508 (2005).
[63]J. Zhang, L. Y. Li, H. K. Tsao, Y. J. Sheng, S. F. Chen, and S. Y. Jiang, Biophys. J. **89**, 158 (2005).